Pancreatology 22 (2022) 294–303

Contents lists available at ScienceDirect

Pancreatology

journal homepage: www.elsevier.com/locate/pan

Sca-1 is a marker for cell plasticity in murine pancreatic epithelial cells and induced by IFN-β in vitro

Georg Leinenkugel [a, *], Bo Kong [g], Susanne Raulefs [b], Katharina Miller [b], Susanne Roth [c], Hongdie Jiang [c], Rouzanna Istvánffy [b], Hanna Heikenwälder [c], Nadja Maeritz [b], Ivonne Regel [d], Ivane Abiatari [e], Jörg Kleeff [f], Christoph W. Michalski [g], Simon Rieder [f]

[a] Department of Gastroenterology and Hepatology, University Hospital Zurich, Switzerland
[b] Department of Surgery, University Hospital of the Technical University, Munich, Germany
[c] Department of Surgery, Heidelberg University Hospital, Heidelberg, Germany
[d] Department of Medicine II, University Hospital, LMU Munich, Munich, Germany
[e] Institute of Medical and Public Health Research, Ilia State University, Tbilisi, Georgia
[f] Department of Visceral, Vascular and Endocrine Surgery, Martin Luther University Hospital, Halle (Saale), Germany
[g] Department of General and Gastrointestinal Surgery, Ulm University Hospital, Ulm, Germany

ARTICLE INFO

Article history:
Received 18 September 2021
Received in revised form
16 November 2021
Accepted 11 January 2022
Available online 13 January 2022

Keywords:
Pancreatic progenitor cells
Interferon
Sca-1
Lin$^-$Sca-1$^+$ hematopoietic stem cells

ABSTRACT

Background & aims: Sca-1 is a surface marker for murine hematopoietic stem cells (HSCs) and type-I interferon is a key regulator for Lin$^-$Sca-1$^+$ HSCs expansion through Ifnar/Stat-1/Sca-1-signaling. In this study we aimed to characterize the role and regulation of Sca-1$^+$ cells in pancreatic regeneration.
Methods: To characterize Sca-1 in vivo, immunohistochemistry and immunofluorescence staining of Sca-1 was conducted in normal pancreas, in cerulein-mediated acute pancreatitis, and in Kras-triggered cancerous lesions. Ifnar/Stat-1/Sca-1-signaling was studied in type-I IFN-treated epithelial explants of adult wildtype, Ifnar$^{-/-}$, and Stat-1$^{-/-}$ mice. Sca-1 induction was analyzed by gene expression and FACS analysis. After isolation of pancreatic epithelial Lin$^-$Sca-1$^+$cells, pancreatosphere-formation and immunofluorescence-assays were carried out to investigate self-renewal and differentiation capabilities.
Results: Sca-1$^+$ cells were located in periacinar and periductal spaces and showed an enrichment during cerulein-induced acute pancreatitis (23.2/100 μm^2 ± 4.9 SEM) and in early inflammation-mediated carcinogenic lesions of the pancreas of Kras^{G12D} mice (35.8/100 μm^2 ± SEM 1.9) compared to controls (3.6/100 μm^2 ± 1.3 SEM). Pancreatic Lin$^-$Sca-1$^+$ cells displayed a small population of 1.46% ± 0.12 SEM in FACS. In IFN-β treated pancreatic epithelial explants, *Sca-1* expression was increased, and Lin$^-$Sca-1$^+$ cells were enriched in vitro (from 1.49% ± 0.36 SEM to 3.85% ± 0.78 SEM). Lin$^-$Sca-1$^+$ cells showed a 12 to 51-fold higher capacity for clonal self-renewal compared to Lin$^-$Sca-1$^-$ cells and generated cells express markers of the acinar and ductal compartment.
Conclusions: Pancreatic Sca-1$^+$ cells enriched during parenchymal damage showed a significant capacity for cell renewal and in vitro plasticity, suggesting that corresponding to the type I interferon-dependent regulation of Lin$^-$Sca-1$^+$ hematopoietic stem cells, pancreatic Sca-1$^+$ cells also employ type-I-interferon for regulating progenitor-cell-homeostasis.

1. Introduction

The last decade saw a marked increase in the depth of understanding of pancreatic organogenesis. It has become apparent that the transition of stem cells into multipotent endodermal pancreatic progenitor cells in the early phase of foregut formation is a crucial step. The underlying regulatory network includes transcription-factors like Pdx-1, Ngn 3, Wnt/β-catenin and Notch-signaling

Abbreviations: ADM, acinar-to-ductal metaplasia; AP, acute pancreatitis; FACS, fluorescence-activated cell sorting; FFPE, formalin-fixed paraffin-embedded; HSC, hematopoietic stem cell; LSK, Lin$^-$Sca-1$^+$c-Kit$^+$; PanIN, pancreatic intraepithelial neoplasia; PDAC, pancreatic ductal adenocarcinoma; PEM, pancreatic epithelial medium; PMM, pancreatic minimal medium; PSM, pancreatic stromal medium; qRT-PCR, quantitative reverse transcription polymerase chain reaction; RT-PCR, qualitative reverse transcription polymerase chain reaction; UPL, universal probe library; WT, wild type.

* Corresponding author. Department of Gastroenterology and Hepatology, University Hospital Zurich, Rämistrasse 100, 8091, Zurich, Switzerland.
E-mail address: georg.leinenkugel@usz.ch (G. Leinenkugel).

https://doi.org/10.1016/j.pan.2022.01.006

[1–5]. However, less is known about the regulation of cell turnover in the adult mammal pancreas. Knowledge about cell-renewal in adult pancreata is of great interest due to their potential role in beta-cell replacement as a treatment for diabetes. There is also evidence that tissue injury, cell plasticity, and transformation to pancreatic ductal adenocarcinoma (PDAC) are linked with each other [6]. Transgenic mice models showed that mature unipotent cells can adopt multipotent function during tissue injury and thus are capable of generating different lineages within the same compartment. One of these processes is acinar-to-ductal metaplasia (ADM), which describes the conversion of acinar cells to a duct-like phenotype [7]. Kopp et al. showed that this de-differentiation process is a key driver of early pancreatic carcinogenesis [8]. Experimental pancreatitis induced by the cholecystokinin-analogue cerulein is a method leading to a de-differentiation of acinar cells making them more permissive for malignant transformation [8]. It is consistently shown that pancreatic epithelial cells are more susceptible for Kras-mediated transformation in the presence of acute or chronic inflammation through interactions between the inflammatory microenvironment and oncogenic Kras [9–11]. One well established mouse model of inflammation-accelerated Kras-driven pancreatic carcinogenesis is the cerulein treatment of $Kras^{G12D}$ mice [12].

It remains controversial if all adult acinar cells keep the plasticity for de- or transdifferentiation or whether this function is confined to a specific compartment of differentiated cells with progenitor properties. In this manner, progenitor cell theories are confronted with genetic lineage-tracing studies, indicating that postnatal β-cells as well as acinar cells arise by duplication of their mature pre-existing cell type and also by metaplastic conversion of one cell type to another without existence of a progenitor like phenotype [13–15].

A variety of pancreatic cell types have been identified to possess progenitor features, including Pdx-1 positive cells dedicated to serve as islet progenitors, Sox-9-positive cells in the ductal compartment, and Nestin-positive cells in the centroacinar area [16–18]. Centroacinar cells can differentiate into exocrine and endocrine lineages in vivo and show high levels of Aldh1a1 enzymatic activity while expressing progenitor markers such as Pdx-1 and Nestin but also c-Kit and Sca-1 [18].

Sca-1 is an 18 kDa phosphatidylinositol-anchored surface protein of the Ly-6 family with so far no direct human ortholog. In mice, together with the tyrosine kinase c-Kit, it is an established marker to identify hematopoietic stem cells (HSCs). The murine Sca-1^+-HSC-population is either labeled as $Lin^-Sca\text{-}1^+c\text{-}Kit^+$ (LSK) population or $Lin^-Sca\text{-}1^+c\text{-}Kit^-$ depending on the status of co-expression with c-Kit. $Lineage^-(Lin^-)$ cells do not express mature hematopoietic lineage markers. The regulatory elements of $Lin^-Sca\text{-}1^+$ HSCs have been characterized: *Sca-1* expression can be induced by type-I-Interferon (IFN-α) mediated by Ifnar/Stat-1 signaling [19,20]. This induction changes HSCs from a quiescent to a proliferative state [20]. Sato et al., 2009 identified the canonical Ifnar/Stat-1 signaling to be crucial for hematopoietic stem cell activation [19]. This effect was measurable when mice were treated with IFN-α in the short term. There is evidence that Interferon/Ifnar/Stat-1signaling exists in rat-derived pancreatic epithelial cells [21], but it remains elusive whether this pathway has a regulatory function for the expansion of pancreatic Sca-1^+ cells in congruency to $Lin^-Sca\text{-}1^+$ HSCs. Moreover, it was shown that $Lin^-Sca\text{-}1^+$ HSCs with high *Sca-1* expression achieved higher rates of self-renewal compared to $Lin^-Sca\text{-}1^+$ HSCs with low *Sca-1* expression [22]. Subsequently, *Sca-1* expression was identified to be conserved in various non-hematopoietic tissues, including prostate, mammary gland, kidney, muscle, cardiac tissue, and skin [23]. Repopulation-assays following FACS of $Lin^-Sca\text{-}1^+$ cells predicted a highly proliferative cell population capable of restoring tubular structures in the kidney and prostate and generating epithelial outgrowth in the mammary gland [24–26]. Sca-1^+ cells derived from primary mammary gland cells also showed tumor-initiating ability in vivo [27].

Moreover, *Sca-1* and *c-Kit* expression could also be identified in the murine pancreas and during pancreatic organogenesis. *c-Kit* is co-expressed with *Pdx-1* and *Ngn3* in the embryonic pancreas, while *Sca-1* shows co-expression with *Pdx-1* and *Ngn3* in the adult organ [28]. Seaberg et al. identified the Sca-1 surface marker in a subset of 9% of islet and 15% of ductal cells [29,30]. In vitro assays by Samuelson et al. [28] revealed high proliferative capability and functional ability for insulin-secretion in Sca-1^+ cells. However, the capacity for self-renewal of this distinct population in adult pancreatic tissue has not been elucidated, so far.

In this study, we investigated the expression of pancreatic Sca-1 in normal pancreata, during regeneration of cerulein-induced acute pancreatitis (AP) of WT mice and in the early cerulein-accelerated carcinogenesis-permissive environment of $Kras^{G12D}$ mice. Further, we studied the role of IFN/Stat-1 signaling in induction of Sca-1 expression in WT, $Ifnar^{-/-}$, $Stat\text{-}1^{-/-}$ derived pancreatic epithelial explants. We then isolated pancreatic Sca-1 cells within the epithelial explants by excluding mature hematopoietic cell surface markers (Lin^-). Lastly, we studied the capacity for self-renewal and differentiation of pancreatic $Lin^-Sca\text{-}1$ with and without co-expression with c-Kit. Unlike the studies for HSC-activation, we used IFN-β instead of IFN-α for technical reasons. IFN-β is mentioned to achieve the same IFN-receptor-affinity and similar biochemical effects. For this reason, we assumed comparable results.

2. Methods

2.1. Mouse lines

$IFN\alpha/\beta R^{-/-}$ (A129) mice on the 129S6/SvEv background were purchased from B&K Universal (Hull, Great Britain). $Stat\text{-}1^{-/-}$ mice on C57Bl/6 background were kindly provided by Bernhard Holzmann (Technical University Munich, Germany). $P48^{+/-Cre}$; LSL-$Kras^{G12D}$ mice (hereafter referred to as '$Kras^{G12D}$ mice') were generated by crossing a strain containing the Lox-STOP-Lox-$Kras^{G12D}$ (LSL-$Kras^{G12D}$; Jax Lab: 008179) gene with mice carrying the pancreas-specific Cre-recombinase $Ptf1a^{+/-Cre}$ (also known as $P48^{+/-Cre}$), courtesy of Roland M. Schmidt and Jens T. Sieveke (Department of Gastroenterology, TU Munich). C57BL/6 wildtype (WT) mice were purchased from Charles River Laboratories (Sulzfeld, Germany). All animal experiments were performed according to regulatory standards and approved by the government of Bavaria (animal experiment permit No. 55.2-1-54-2532-147-09).

2.2. In vivo cerulein treatment

Induction of pancreatitis was performed on 8–10 week old WT and $Kras^{G12D}$ mice through 8 hourly intraperitoneal injections of 50 μg/kg body weight cerulein (Sigma Aldrich) in 100 μl 0.9% physiological saline on 2 consecutive days. This protocol is in accordance to the previously described "consecutive" protocol [31]. Healthy control mice received placebo injections of 100 μl physiological saline. Analgesia was conducted with buprenorphin (0.1 mg/kg body weight) before the first cerulein injection. Animals were sacrificed 1 h (WT) and 14 days ($Kras^{G12D}$ mice) after the final cerulein injection and pancreata were harvested for further analysis. 1 h after the final day of cerulein injection was considered as day 3.

2.3. Pancreatic epithelial and stromal cell explants in suspension and 2D-culture

Epithelial cells were obtained as previously described with minor modifications [32]. Pancreatic stromal cells were separated from the epithelial cell fraction using a modified method from the "outgrowth protocol" as described [33]. Floating pancreatic epithelial cells were incubated in Pancreatic Epithelial Medium (PEM) for a minimum of 4 h after harvesting and subjected to IFN-β-treatment-experiments or FACS analysis. Adherent pancreatic stromal cells were thawed and cultured until 70% confluency before IFN-β treatment experiments (mean cultivation time after explantation 22 days).

2.4. Cell culture media (PEM/PSM/PMM)

See detailed methods and materials section.

2.5. In vitro IFN-β treatment

IFN-β (Interferon-beta 1a) was obtained in a concentration of 5×10^4 international units per milliliter (IU/ml) by Hycult-Biotech (Uden, Netherlands). Previous in-vitro studies showed that interferon in a range between 100 and 1000 IU/ml is sufficient to induce antiproliferative effects [34]. IFN-β was therefore used in lower concentrations of 100 IU/ml if not otherwise stated. It was directly applied into the culture medium. Pancreatic epithelial, stromal and Lin$^-$Sca-1$^+$ cells were treated with IFN-β for different time points of 4 h, 24 h (day 1), 48 h (day 2) and 144 h (day 6) and afterwards subjected to qRT-PCR or FACS. Treatment of Lin$^-$Sca-1$^+$cells was repeated every 48 h together with media-change.

2.6. RNA isolation and cDNA synthesis, qualitative-PCR (RT-PCR) and quantitative-PCR (qRT-PCR)

See detailed methods and materials section.

2.7. FACS analysis of Lin$^-$Sca-1$^+$ and Lin$^-$Sca1$^-$c-Kit$^+$ cells

The single-cell suspension of the pancreatic epithelial explants was stained with Sca-1, c-Kit and biotine conjugated lineage panel including B220, CD11B, GR1, TER119, CD3E for 15 min at 4 °C in 1x PBS and 0.5% FCS. Cell populations were sorted according to the sorting scheme using FACSAria Cell Sorting System (BD). Regarding the Lin$^-$c-Kit$^+$ Sca1$^+$ cell populations, two c-Kit$^+$ populations with high and medium expression of Sca-1 and c-Kit were separated and sorted for the further analysis.

2.8. Quantitative pancreatosphere formation assay

Pancreatosphere formation assay of sorted Lin$^-$Sca-1$^+$ and Lin$^-$Sca1$^-$c-Kit$^+$ cells was performed by plating sorted cells in 24-well ultra-low attachment plates (Corning) at densities of 100, 1000 and 2400 cells per well in Pancreatic Minimal Medium (PMM). Cells were grown for 6 days if not stated otherwise, and sphere formation was quantified using an Axiovert 40 CFL microscope (Carl Zeiss).

2.9. Lin$^-$Sca-1$^+$-3D-culture

Matrigel™-coated chamber slides (BD) were used for immunofluorescence analysis or light microscopy of Lin$^-$Sca-1$^+$ or Lin$^-$Sca-1$^+$ c-Kit$^+$ cells- and spheres after cultivation of 5–14 days.

2.10. Histology, immunohistochemistry, and immunofluorescence

For histological analysis, 3.5 μm thick tissue sections from paraffin-embedded tissue blocks were stained with hematoxylin and eosin (H&E) according to standard procedures. Immunohistochemistry staining was performed using affinity-purified polyclonal antibodies followed by color reaction with the DAB+ Substrate Chromogen System (Dako, Hamburg, Germany) or the AEC+ High Sensitivity Substrate Chromogen (Dako). Light microscope pictures were taken with an Axioscope microscope (Zeiss). Immunofluorescence staining of Matrigel™-coated slides was conducted using standard protocols. Fluorescent images were obtained with the Axioscope microscope (Zeiss). Immunofluorescence staining of Sca-1 and pStat-1 in WT native pancreas, cerulein-induced acute pancreatitis, and Kras^{G12D} mice formalin-fixed paraffin-embedded (FFPE) tissue sections was done as described previously [11]. Images were obtained with a BZ-900 KEYENCE all-in-one fluorescence microscope. Quantification of Sca-1/pStat-1 antibody staining was performed by examining 1.7 mm^2 tissue areas per slide and semi-automated counting of Sca-1/pStat-1 positive cells using ImageJ software (NIH, Bethesda).

2.11. Statistical analysis

Data are presented as mean ± SEM or median ± interquartile range. Statistical significance was determined by *one-way* analysis *of variance* (Anova) or unpaired Student's *t*-test as indicated in the figure legends using GraphPad Prism 9.1 software (GraphPad Software Inc.) or R (R Core Team). *P* values less than 0.05 were considered significant.

2.12. Detailed methods and materials

A detailed methods and materials section is provided as a supplement to this manuscript.

3. Results

3.1. Sca-1 expression is induced during regeneration of WT acute pancreatitis and inflammation-accelerated carcinogenic pancreas of Kras^{G12D} mice in vivo

First, we assessed Sca-1 expression and location in the pancreas of 8–10 week old WT mice. In normal pancreas, Sca-1$^+$ cells were located close to ducts, lining their epithelium and distributed in the periacinar space (Fig. 1A). The Sca-1-staining-pattern did not reveal substantial overlap to ductal CK-19, indicating no direct ductal progeny (Fig. 1B). Next, we compared normal pancreas with the tissue of disturbed integrity out of inflammatory as well as carcinogenic-altered-pancreas. Quantitative Sca-1 immunofluorescence was performed on bulk-tissue of 8–10 week old mice normal pancreas (Control), cerulein-induced acute pancreatitis (AP), and cerulein-accelerated Kras-induced carcinogenic pancreas of Kras^{G12D} mice (Kras^{G12D}). Co-staining of pStat-1 and Sca-1 was conducted to investigate whether Ifnar/Stat-1 signaling is activated during states of reduced tissue integrity (Fig. 1C and D). In acute pancreatitis, we quantified Sca-1$^+$ cells on day 3 in the early regenerative phase of cerulein-induced pancreatitis. In 8-week-old mice, the pancreas regains normal histology within one week after cerulein treatment. In the early phase (day 1–2) of pancreatitis, edema, apoptosis with massive exocrine cell loss, and immune cell infiltration is seen. Increased mitotic activity is mainly seen in interstitial cells. Later states following day 3 include highly increased mitotic activity in exocrine cells and stromal expansion [35,36]. In our study, Sca-1$^+$ cells were 6.4 times enriched (23.2/

100 μm^2, SEM 4.9) in pancreata of acute pancreatitis on day 3 after cerulein treatment in relation to Sca-1$^+$ cells of controls (3.6/100 μm^2, SEM 1.3) (Fig. 1C). Between the first 3 days histological pattern of acute pancreatitis in WT and Kras^{G12D} mice are considered to be similar to those of WT mice. Pancreata of 7–14 days old cerulein-treated Kras^{G12D} mice are known to be in the early transformation-state showing preneoplastic lesions [11]. We therefore quantified Sca-1$^+$ cells on day 14 of cerulein-treated Kras^{G12D} pancreas. Next to ADM lesions of ductal phenotype, lobular fibrosis as well as atypical flat lesions (putative PDAC precursors) and scattered low-grade intraepithelial neoplasia (PanINs) located in atrophic areas were noted (Fig. 1D). In this state Sca-1$^+$ cells were drastically enriched (9.9 times, 35.8/100 μm^2, SEM 1.9) compared to controls (3.6/100 μm^2, SEM 1.3), and 1.5 times compared to tissue of the regeneration phase after acute pancreatitis (23.2/100 μm^2, SEM 4.9) (Fig. 1C). Sca-1$^+$ cells were co-localized mainly with atypical ductal epithelial cells (Fig. 1D). Surprisingly, pStat1$^+$ staining patterns during regeneration after acute pancreatitis or inflammation-accelerated carginogenic pancreas of Kras^{G12D} mice did not show increased pStat-1-levels compared to normal pancreas (Fig. 1C). This result questions the role of pStat-1 for Ifnar-Sca-1-signaling during the expansion of pancreatic Sca-1$^+$ cells in general.

Altogether, Sca-1 is expressed in a close neighborhood to ducts and acinar cells. Sca-1$^+$cells are enriched in the phase of regeneration after acute pancreatitis and during early pancreatic carcinogenesis. However, pStat-1 was unaltered during regeneration after cerulein induced acute pancreatitis and in inflammation-accelerated carcinogenic pancreas of Kras^{G12D} mice, which might indicate a Stat-1 independent Sca-1 induction in Sca-1$^+$ pancreatic cells. These results diverge from the known canonical Ifnar-Stat-1 pathway in Lin$^-$Sca-1$^+$ HSCs.

3.2. IFN-β induces pancreatic Sca-1 expression and enriches pancreatic Lin$^-$Sca-1$^+$ cells in vitro

Next, we wanted to determine in more detail whether Ifnar-Stat-1-Sca-1 induction exists in pancreatic cells in vitro by studying primary pancreatic cell explants in suspension and 2D-culture treated with IFN-β. Existing data claimed Sca-1 also to be expressed on mesenchymal and stromal, and not only on epithelial cells [23]. Pancreatic regeneration studies reveal high mitotic activity mainly in the exocrine compartment but in the early phase also in interstitial cells [36]. To localize in which pancreatic compartment IFN-Sca-1 reactivity occurs, we included primary epithelial-as well as 22 days old (mean) stromal explants of 8–10 week old WT mice pancreata. 4 h and 2 days old epithelial explants in suspension-culture were validated by RT-PCR, revealing mostly expression of epithelial markers and a small band for *vimentin* not excluding low-grade stromal-cell cross-contamination.

Light microscopy confirmed most cells to be of acinar origin (Fig. 1E). Primary pancreatic stromal explants on day 22 in 2D-culture displayed polygonal fibroblast configuration and expressed stromal markers (Fig. 1E). In epithelial cells, a hematopoietic surface marker *Ptprc* [CD45] was measured to rule out hematopoietic-cell-contamination (Fig. 1E). Before we checked for Sca-1 expression, we investigated functionality of Ifnar-Stat-1-signaling in epithelial cells. Therefore, we quantified the expression levels of the conventional IFN-Ifnar-Stat-1 inducible chemokines *Cxcl-10* and *Cxcl-11* after 4 h IFN-β treatment in pancreatic epithelial explants of WT and Stat-1$^{-/-}$ mice. Our data indicated an IFN-β dose-dependent upregulation of *Cxcl-10*, *Cxcl-11* in WT- but not Stat-1$^{-/-}$ epithelial explants (Fig. 1F). Together with literature recommendations, this data was used to establish the IFN-β dose applied in the following IFN-β-Sca-1 treatment experiments (Fig. 2 A + E).

In this context, we measured *Sca-1* expression after 1 day IFN-β treatment of pancreatic epithelial and stromal explants revealing significant expression-induction in epithelial cells. Stromal explants however, did not show IFN-β mediated *Sca-1* expression at all (Fig. 2B). Next, we analyzed whether IFN-β might upregulate other established progenitor markers in pancreatic epithelial explants as well. Expression levels of *Pdx1*, *c-Kit* and *Aldha1a* were also elevated in vitro on day 1 and 2 culture (Fig. 2C). Nevertheless, this seemed to be IFN-β independent. Further, we could not find

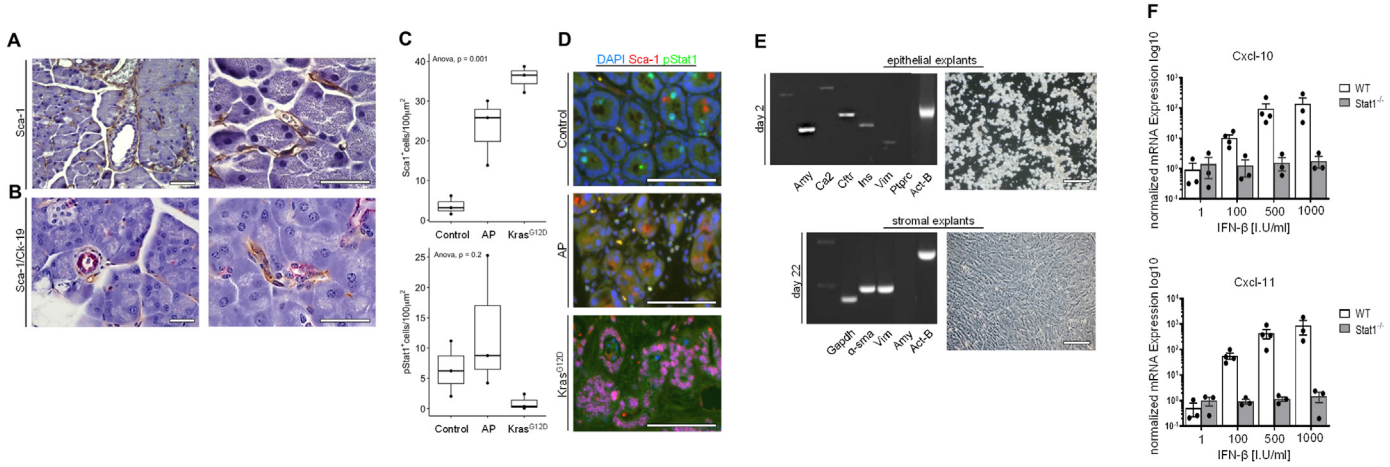

Fig. 1. IFN-β-Stat-1 sensitivity of pancreatic epithelial cells. Sca-1expression is induced after WT acute pancreatitis and inflammation-accelerated carcinogenic pancreas of Kras^{G12D} mice in vivo. (A–B) IHC staining for Sca-1 (brown) (A) and Sca-1 (brown)/Ck-19 (purple) (B) in paraffin-embedded section of pancreas in 8–10 week old WT mice. Sca-1$^+$cells were located in the periacinar and periductal space without substantial overlap expression to ductal CK-19. Axioscope, magnification 200–400x scale bar: 50 μm. (C–D) Quantification of Sca-1$^+$cells and pStat-1$^+$cells per 100 μm^2 in immunofluorescence staining of 8–10 week old control, AP (day 3 after cerulein treatment) and pancreata of Kras^{G12D} mice (day 14 after cerulein treatment) (n = 3) (D). Representative pictures of immunofluorescence staining of Sca-1 and pStat-1 in Control, AP and Kras^{G12D} pancreatic tissue samples. BZ-900 KEYENCE, magnification: 200x, scale bar 100 μm. (E) Representative picture and RT-PCR for epithelial (*Amy, Ca2, Cftr, Ins*), stromal (*Vim*), and hematopoietic marker *Ptprc* (*Cd45*) in pancreatic epithelial explants on day 2. Representative picture and RT-PCR of stromal (*Vim*, *α-sma*) and acinar (*Amy*) in stromal explants on day 22. Axioscope, magnification 20x scale bar: 100 μm (F) Expression levels of *Cxcl-10* and *Cxcl-11* after IFN-β-treatment in 4 h old pancreatic epithelial explants of WT- and Stat-1$^{-/-}$ mice normalized to housekeeping genes (IFN-β-dose: 1–1000 I.U/ml) (n = 3–4). Data are presented as mean mean ± SEM. p-values were calculated with unpaired Student's t-test and ANOVA, respectively.

induction of *Nestin*, *Ptf1a1* and *C-met* (Fig. 2D).

In order to determine whether pancreatic Sca-1 expression is a downstream-target of Ifnar-Stat-1-signaling in correspondence with Lin$^-$Sca-1$^+$ HSCs, we performed the same IFN-β treatment on epithelial explants of Ifnar$^{-/-}$ mice and Stat-1$^{-/-}$ mice (Fig. 2E). The data indicated no Sca-1 induction following IFN-β treatment in pancreatic epithelial Ifnar$^{-/-}$ cells, while Sca-1 expression was upregulated in pancreatic Stat-1$^{-/-}$ cells (Fig. 2F). According to this data, Ifnar but not Stat-1 is the relevant factor for pancreatic IFN-β-Sca-1-signaling.

To further characterize the Sca-1$^+$ cell population within the epithelial explants, we sorted Lin$^-$Sca-1$^-$ and Lin$^-$Sca-1$^+$ cell population gated on alive PI$^-$ cells from WT-epithelial explants according to the sorting scheme (Fig. 2G). In brief, we primarily gated out cell debris and PI$^+$ dead cells, shown in the FACS plots from the upper panel. Further, we gated in Lin$^-$ fraction Sca-1$^+$ and Sca-1$^-$ cells (Fig. 2G). Interestingly, in fraction of Lin$^-$Sca1$^+$ cells showed high expression of c-Kit, similarly with the phenotype of c-Kit in Lin$^-$Sca-1$^+$ c-Kit$^+$ HSCs (LSKs) (Fig. 2G). On day 1 after extraction, Lin$^-$Sca-1$^+$ cells represented a distinct population of 1.46% (0.12 SEM) of all sorted cells (Fig. 2H). Epithelial explants, treated with IFN-β for 2 days, led to enrichment of the Lin$^-$Sca-1$^+$cell-fraction to a subset of 3.85% (0.78 SEM) of all sorted cells. The untreated control on day 2 represented a population of 2.85% (0.29 SEM) of the overall population (Fig. 2I). This means Sca-1$^+$ cell population is enriched during time-course of suspension culture which can be accelerated by IFN-treatment. Interestingly *Ifnar*-1 chain RNA of the interferon receptor in day 2 epithelial Lin$^-$Sca-1$^+$ explants was nearly 4 times higher expressed than in Lin$^-$Sca-1$^-$ explants (Fig. 2J). This could indicate increased IFN-sensitivity of the Lin$^-$Sca-1$^+$cell population.

To summarize, pancreatic Lin$^-$Sca-1$^+$ cells are reactive to IFN-Sca-1-signaling. This effect is an attribute in epithelial but not stromal cells in vitro. The molecular mechanisms underlying this signaling pathway are likely similar to the interferon signaling in Sca-1$^+$ HSCs.

3.3. Lin$^-$Sca-1$^+$ cells show increased capacity of self-renewal in vitro. Lin$^-$Sca-1$^+$ cells can generate pancreatic exocrine and ductal lineages in 3D-culture

To determine self-renewal-capabilities of pancreatic Lin$^-$Sca-1$^+$cells we performed quantitative pancreatosphere-formation assays. This technique is used to profile pancreatic progenitor cells [18,30] and is derived from the neurosphere-assay to identify neural progenitors [37]. We sorted Lin$^-$Sca-1$^-$ and Lin$^-$Sca-1$^+$ cell populations of WT epithelial explants with the above described sorting-strategy and plated them in defined serum-free-media conditions (PMM) at different cell densities. By day 6, floating colonies resembling pancreatospheres were quantified. The results showed that the number of spheres formed in both populations differed significantly. The sphere forming capacity was 12–51 fold increased in Lin$^-$Sca-1$^+$ cells compared to Lin$^-$Sca-1$^-$cells depending on the plated cell density (e.g.: 2400 cells/well, day 6: Lin$^-$Sca-1$^+$: 1/470 vs. Lin$^-$Sca-1$^-$: 1/24000, spheres/cells) (Fig. 3A+B).

In correspondence to Sca-1 co-expression of the tyrosine kinase c-Kit in Lin$^-$Sca-1$^+$ c-Kit$^+$ HSCs (LSKs), we also investigated co-expression of Sca-1 and c-Kit in pancreatic epithelial explants together with its capability of self-renewal. Epithelial cell explants on day 1 showed co-expression of Sca-1 and c-Kit in a minimal subset of 0.1% of all sorted cells (Fig. 3C). The capacity to form spheres in Lin$^-$Sca-1$^+$c-Kit$^+$ and Lin$^-$Sca-1$^+$c-Kit$^-$ cells was more enhanced compared to Lin$^-$Sca-1$^-$ -/and Lin$^-$c-Kit$^-$cells. Lin$^-$c-Kit$^+$ explants did not form significantly more spheres than Lin$^-$ cells not expressing Sca-1 and c-Kit, neither enhanced c-Kit the sphere forming capacity in Lin$^-$Sca-1$^+$c-Kit$^+$ cells (Fig. 3D). This indicates that Sca-1 and not c-Kit could be the crucial antigen marker, labeling cells with increased self-renewal-properties. However if IFN-β was administered in high-dose and chronically (1000 I.U/ml; 6 days) to pancreatic Lin$^-$Sca-1$^+$ cells, sphere formation capacity decreased rapidly (Fig. 3E).

To determine the differentiation capability of pancreatic Lin$^-$Sca-1$^+$ colonies, we separated clonal floating Lin$^-$Sca-1$^+$ colonies and plated them in adherent 3D-culture environment. In 3D-culture, Lin$^-$Sca-1$^+$cells generated larger spheres as in serum-free-media-suspension culture (Fig. 3F). In 5–14 days culture, Lin$^-$Sca-1$^+$ cells formed colonies in complex tubular-elongated polarity. Immunofluorescence-studies of these colonies showed expression of epithelial E-Cadherin, Amylase, Ck-19. A subset of these cells stained positive for Nestin (Fig. 3G). Chemical dissociation and replating of Lin$^-$Sca-1$^+$ spheres grown in 3D-culture led to the generation of small secondary spheres. They underwent growth stagnation after 7–14 days, indicating limited self-renewal-capacity in this culture condition.

In summary, our data indicate that in similarity to Lin$^-$Sca-1$^+$ HSCs (LSKs), pancreatic epithelial Lin$^-$Sca-1 cells are capable of clonal-self renewal and differentiation into cells expressing acinar and ductal markers. They are inducible through IFN-β in an Ifnar- but not Stat-1-dependent manner and are enriched during phases of regeneration in acute pancreatitis and early inflammation driven pancreatic carcinogenesis.

4. Discussion

To regain tissue homeostasis following acute pancreatitis, the capability to replace functional cells within a short period is essential [38]. Persistent inflammatory tissue damage activates regenerative mechanisms, which seem to include the expansion of pancreatic progenitor cells [6]. A profound understanding of cellular plasticity includes knowing pancreatic precursor cells and their associated regulating signaling networks. This knowledge might be the key for pancreatic-cell-replacement-therapies and might offer targets for specific anti-proliferative-therapies in pancreatic cancer. In the adult pancreas, progenitor-like-cells can be isolated by FACS using a variety of cell surface-markers like Aldha1a, Pdx1, Nestin, Ptf1a1, and C-met [39]. Emerging knowledge of striking similarities between HSCs and tissue-resident-progenitor-cells led to the question whether surface markers labeling HSCs might also be markers of stem and progenitor-cells in non-hematopoietic tissue. One of these markers found in HSCs is Sca-1, present in Lin$^-$Sca-1$^+$ HSCs and pancreatic derived progenitor-like cells [18,28,30]. It is unknown whether pancreatic Lin$^-$Sca-1$^+$ cells also share similarities in the paracrine IFN-α dependent regulatory pathway of Lin$^-$Sca-1$^+$ HSCs [19,20]. Furthermore, their ability for clonal self-renewal and differentiation was not addressed conclusively until now.

In the present study, we identified a pancreatic cell population expressing Sca-1 that is enriched during regeneration of cerulein-induced AP and in presence of early inflammation accelerated oncogenic Kras^{G12D}. Sca-1 expression could be induced in pancreatic epithelial explants in vitro, linked together with an enrichment of Lin$^-$Sca-1$^+$cells. IFN-β was mediating this induction similar to the Lin$^-$Sca-1 hematopoietic counterpart in an Ifnar-dependent manner.

Our in vivo expression analysis revealed that Sca-1 cells reside in the close proximity of the junctional area of ducts and the periacinar region. Functionally, the Ifnar-Sca-1 pathway could not be induced in pancreatic stromal cells. Further no significant overlap of Sca-1 to ductal-CK-19 was detected as previously described by Samuelson et al. [28]. This raises the question whether this population is of exocrine progeny or shows similarities to centroacinar or

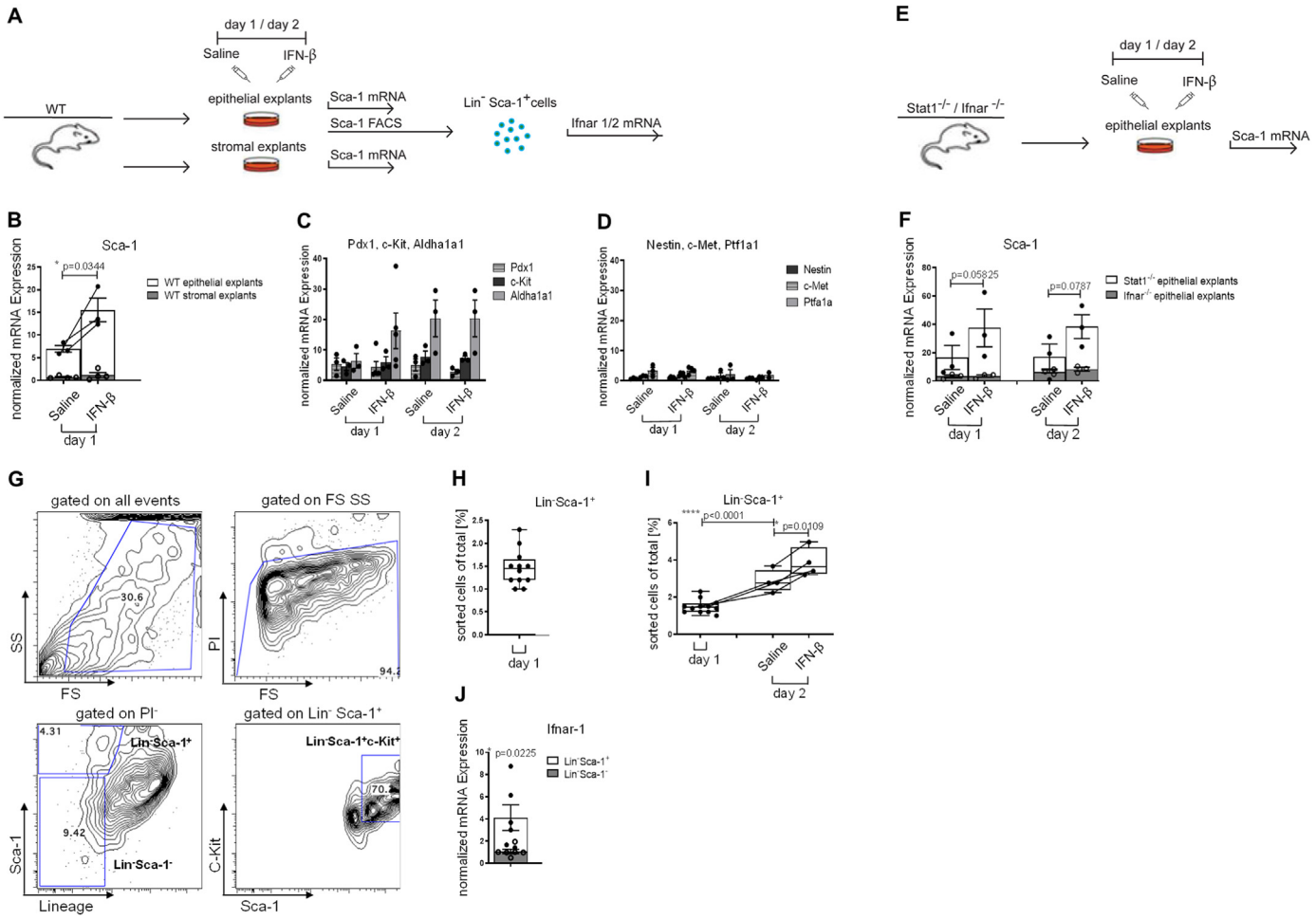

Fig. 2. IFN-β induces pancreatic Sca-1 expression and enriches pancreatic Lin⁻Sca-1⁺ cells in vitro. (A) Visualization of IFN-β-treatment experiments in pancreatic epithelial and stromal explants of WT mice. (B) *Sca-1* expression levels in pancreatic epithelial and stromal explants on day 1 after IFN-β-treatment compared to saline (n = 3–4). (C–D) Expression levels of *c-Kit*, *Nestin*, *C-met*, *Ptf1a1*, *Pdx1*, *Aldh1a1* in pancreatic epithelial explants of WT mice on day 1 and day 2 after treatment with IFN-β compared to saline and normalized to housekeeping genes (n = 3–5). (E) Visualization of IFN-β-treatment experiments in pancreatic epithelial explants of Ifnar$^{-/-}$ and Stat-1$^{-/-}$ mice. (F) *Sca-1* expression levels in pancreatic epithelial explants of Ifnar$^{-/-}$ and Stat-1$^{-/-}$ mice on day 1 and day 2 after treatment with IFN-β compared to saline and normalized to housekeeping genes (n = 3). (G) FACS of 4 h old pancreatic epithelial explants using antibodies against Sca-1, c-Kit and biotine conjugated Lineage Panel by gated out depris and PI^{+} dead cells (upper panel) and gated Lin^{-}fraction Sca-1^{+}, Sca-1^{-} and c-Kit^{+}cells (lower panel) (n = 3) (H) FACS for pancreatic epithelial Sca-1 lineage negative cells (Lin^{-}Sca^{+} cells) on day 1 yielded a population of 1.46% (0.12 SEM) of all sorted cells. (I) FACS of Lin-Sca-1^{+}-cells after 2 days of IFN-β-treatment led to enrichment to 3.85% (0.78 SEM) of all sorted cells (n = 4–6). Saline controls were represented by a subset of 2.85% (0.29 SEM) of all sorted cells (n = 5) (J) Expression of IFN-receptor-gene *Ifnar-1* in pancreatic epithelial Lin^{-}Sca-1^{+} compared to Lin^{-}Sca-1^{-} explants normalized to housekeeping genes (n = 5). Data are presented as mean ± SEM/median ± interquartile range (H,I). p-values were calculated with unpaired Student's t-test; *p ≤ 0.05, **p < 0.01, ***p < 0.001, ****p < 0.0001.

terminal duct cells, which have been previously described as capable of transdifferentiation in response to epithelial injury [18,40]. Rovira et al. [18] detected high levels of Sca-1, Aldha1a, C-met and Nestin in centroacinar or terminal duct cells which we could also identify in our pancreatic epithelial explants. However, in regard to Sca-1 cell distribution in the adult pancreas, data are conflicting. Seaberg et al. [30] identified Sca-1^{+} cells in a subset of 9% of islet-cells and 15% of ductal cells in the adult mouse pancreas. In our study, Lin^{-}Sca-1^{+} surface markers were expressed to a much smaller extent of just 1.46% of all digested epithelial cells. However, the extraction method of pancreatic cells by Seaberg's study group was targeting specifically ducts and islets. Therefore, we cannot determine to which extent the extracted Sca-1^{+} population by Seaberg et al. differs from our pancreatic epithelial population. We are aware that our epithelial cell Isolation method has limitations due to low-grade stromal-cell cross-contamination of non-epithelial cells, particularly of stromal origin, as we could show. Gene expression profiling and FACS are necessary to more concise target the origin of murine pancreatic Sca-1 cells. In this respect, it will be essential to uncover overlap-expression between Sca-1 and other markers of previously described progenitor populations in future research. We could detect co-expression of Sca-1 and c-Kit in adult pancreatic epithelial explants revealed by FACS and immunofluorescence-study. It is known that both markers are expressed independently in the embryonic pancreas as shown by Ma et al. [29]. Nevertheless, how and why Sca-1 and c-Kit expression pattern might change in pre- and postnatal pancreas remains unclear and necessitates additional investigation.

We could link type-I-IFN-signaling in pancreatic epithelial explants with Sca-1 enrichment. However, under physiological conditions, type-I-interferons are strong inhibitors of proliferation in general and are pharmaceutically used to treat tumors and viral infections. This effect might seem contradictory to attribute IFNs to play a role in progenitor cell expansion at first sight. If acutely administered, Essers et al. [29] showed that low-dose IFN-α activates Lin^{-}Sca-1^{+} HSCs, promoting proliferation. If IFN-α is

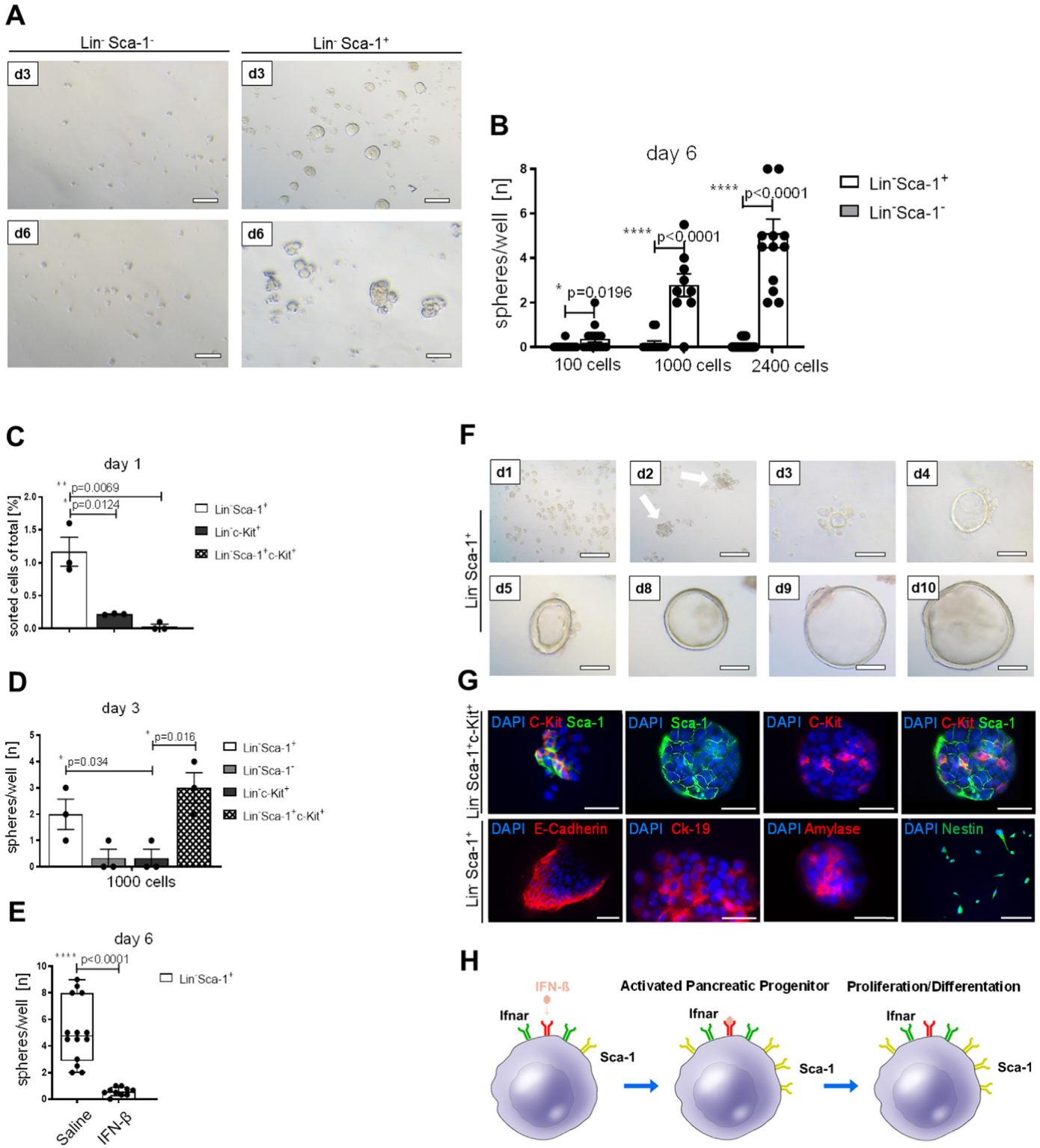

Fig. 3. Lin$^-$Sca-1$^+$ cells cells show increased capacity of self-renewal and can generate pancreatic exocrine and ductal lineages in vitro. (A) Representative picture of pancreatic Lin$^-$Sca-1$^-$ and Lin$^-$Sca-1$^+$ cells and pancreatospheres in PMM on day 3 and day 6 of sphere formation assay. Axioscope, magnification 20x, scale bar: 200 μm. (B) Quantification of pancreatospheres formed by Lin$^-$Sca-1$^+$ cells compared to Lin$^-$Sca-1$^-$ cells on day 6 of sphere formation assay. Plating densities: 100 cells/well, 1000 cells/well, 2400 cells/well (n = 4). (C) FACS of 4 h old pancreatic epithelial explants revealed a subset of 1.16% Lin$^-$Sca-1$^+$ cells, 0.2% Lin$^-$c-Kit$^+$ cells and 0.1% Lin$^-$Sca-1$^+$ c-Kit$^+$cells of all sorted cells (n = 3). (D) Quantification of pancreatospheres formed by Lin$^-$Sca-1$^+$cells, Lin$^-$Sca-1$^-$ cells, Lin$^-$c-Kit$^+$ cells, Lin$^-$Sca-1$^+$c-Kit$^+$cells on day 3 of sphere-formation-assay (n = 3). Plating density: 1000 cells/well. (E) Quantification of pancreatospheres formed by Lin$^-$Sca-1$^+$ cells after 6 days of high-dose IFN-β treatment (1000 I.U/ml) compared to saline (n = 4). (F) Time course of Lin$^-$Sca-1$^+$ pancreatosphere in 3D-culture (Matrigel™) with PMM for 10 days. White arrows show sphere-forming cells. Axioscope, magnification 50–100x, scale bar: 400 μm. (G) 3D-culture (Matrigel™): Immunofluorescence staining of Sca-1 and c-Kit in Lin$^-$Sca-1$^+$ c-Kit$^+$ plane culture and spheroid configuration (day 11). Axioscope, magnification: 100x, scale bar: 50 μm (upper panel). Immunofluorescence staining of Lin$^-$Sca-1$^+$ cells with staining of E-Cadherin on day 5, Ck-19 on day 12, Amylase on day 10, and Nestin on day 14. Axioscope, magnification: 100x, scale bar: 50 μm (lower panel) (H) Our proposed model of IFN-β-Infar-Sca-1-signaling leading to activation of pancreatic Lin$^-$Sca-1$^+$cells in correspondence to the activation of Lin$^-$Sca-1$^+$ HSCs. Data are presented as mean ± SEM/median ± interquartile range (E). p-values were calculated with unpaired Student's *t*-test; *p ≤ 0.05, **p < 0.01, ***p < 0.001, ****p < 0.0001.

administered in high dose or chronically, however, it led to suppressive effects and subsequent exhaustion of HSCs [20]. It remains speculative whether, in most parts of our study, exposure time and dose of IFN-β to pancreatic epithelial cells remained probably under the threshold of exhibiting antiproliferative effects. In this regard, our experiments also revealed that if IFN-β was administered in high-dose and chronically (1000 I.U/ml; 6 days) to pancreatic Lin$^-$Sca-1$^+$ cells, sphere formation capacity decreased rapidly (Fig. 3G). Due to heterogenity of experimental setups, the difference of IFN-Types, dosing, and exposure times used in the literature, this conflicting data in terms of IFN-mediated effects on cell plasticity remains unsolved. IFN-effects likely need to be investigated with more differentiation regarding the time and dose exposure of target cells.

In contrast to the findings of Essers et al., our knock-out-experiments showed Sca-1 induction in pancreatic epithelial explants was not dependent on Stat-1 but Ifnar-signal-transduction. This data was supported by unaltered levels of pStat-1 in tissue of expanding Sca-1$^+$ cells during regeneration of experimental pancreatitis and in carginogenic altered pancreas of Kras^{G12D} mice. However, this result was mainly visible on a gene-expression-level and might require further validation.

Pancreatic Lin$^-$Sca-1$^+$ cells could generate cells expressing markers of the ductal and exocrine lineage and expressed Nestin, which is co-expressed with Sca-1 in a recently described work about putative centroacinar/terminal ductal progenitor cells [18]. We observed a distinctive capacity for clonal self-renewal in pancreatic Lin$^-$Sca-1$^+$ cells and Lin$^-$Sca-1$^+$ c-Kit$^+$ cells. This capacity could not be found in Lin$^-$Sca-1$^-$cells. The sphere forming capacity of Sca-1$^+$cells is described in the literature for Sca-1$^+$cells derived from heart, prostate and mammary gland [24,27,41]. Samuelson et al. [28] could link high proliferative abilities of pancreatic Sca-1$^+$ cells derived from 2 to 3 week old mouse pancreas. However, Seaberg et al. [30] could not detect colony forming ability of pancreatic Sca-1$^+$ cells in serum-free-media derived from 6 week old mice, which is in contrast to our data of Lin$^-$Sca-1$^+$cells derived from 8 to 10 week old mice. A potential explanation for these divergent findings is that previously described differences in cell explanation methods between Seaberg's and our study group might also lead to diverse cell-populations with different sphere forming capacities.

We could show that Sca-1$^+$ cells are expanded during regeneration of acute pancreatitis and during presence of oncogenic Kras^{G12D} and inflammation. Functionally, phenotypic plasticity in vivo can involve de- and transdifferentiation, which inherits a risk for cancer formation. For this reason, a major challenge will be the sufficient characterization of pancreatic Sca-1$^+$ cells in invivo plasticity. Further genetic lineage tracing studies and repopulation-assays of labeled Lin$^-$Sca-1$^+$ cells are needed to understand more precisely the recruitment and repopulation abilities in the micro-environment of inflammation. This could also wipe out potential cell culture artefacts of in vitro characterization. Further experiments also need to focus on its tumor initiating capability.

We also are aware that a direct homolog of Sca-1 in humans is still missing, and the function of the human LY6 gene family is not yet defined. However, even if Sca-1 has yet no direct homolog, a number of potential human homologs for the murine Ly6 family have been identified [42]. Many of the human LY6 genes are highly expressed in tumors, including ovarian, colon, stomach, breast, lung, bladder, brain, and also pancreatic cancers, compared to adjacent normal tissue, reminiscent of the association between Sca-1 and murine cancer-manifestations in mice [43]. Further, there are functional similarities between Sca-1 and other phosphatidylinositol-anchored surface proteins [23]. The identification of a human ortholog or similar proteins could inherit the possibility of a direct transfer of knowledge regarding the mechanisms underlying the function of Sca-1 also in human-stem-cell-homoeostasis [23].

To summarize this study, we demonstrated in vitro plasticity of murine pancreatic Sca-1$^+$ cells and we might have uncovered an essential regulatory signaling pathway. This pathway employs type-I-IFNs as critical components, not only in Lin$^-$Sca-1$^+$ HSCs induction but also in the pancreatic Sca-1$^+$ progenitor cell homeostasis. Further characterization of this population together with further advancements in identifying a human Sca-1 equivalent could reveal the link between immunogenic cytokine-mediated stress-signals, pancreatic tissue regeneration and carcinogenesis and might be useful in the targeted treatment of inflammatory and oncogenic pancreatic diseases.

5. Detailed methods and materials

5.1. Cell culture media (PEM/PSM/PMM)

Pancreatic Epithelial Medium (PEM) consists of DMEM/Ham's F12 (PAA), 10% FCS (PAA), 1% Penicillin/Streptomycin (PAA). Pancreatic Stromal Medium (PSM) consist of a 1:1 (vol/vol) mixture of Dulbecco's modified Eagle medium (DMEM) with Ham's F12 medium, L-Glutamine (2 mmol) (PAA), 10% FCS (PAA), 1% Penicillin/Streptomycin (PAA). Pancreatic minimal Medium (PMM) for experiments that require serum starvation consists of DMEM/Ham's F12 (PAA) supplemented with 20 ng/ml EGF (Sigma-Aldrich), 10 ng/ml FGF 2 (Sigma-Aldrich), 2 μg/ml Heparin (Sigma-Aldrich), 2% B27-Supplement (50x) (Invitrogen), 1% Insulin-Transferrin-Selenium (100x) (Invitrogen), 1% Penicillin-Streptomycin (PAA).

5.2. Pancreatic epithelial explants in suspension-culture

Whole pancreas was harvested from euthanized mice, minced and digested in 1.2 mg/ml of Collagenase 8 (Sigma-Aldrich) at 37 °C for 30 min. After multiple washing steps in McCoy's 5A Medium (PAA) with 5% FCS (PAA) digested-tissue-pieces were filtered through a 100 μm polypropylene-mesh (BD) and washed twice. The cell pellet was resuspended in PEM and cultured for at least for 4 h at 37 °C and 5% CO2. After washing, cells were either subjected to IFN-β -treatment-experiments or FACS analysis. For FACS, pelleted cells were resuspended in diluted trypsin (0.05%) (PAA) and incubated at 37 °C for 15 min. Dispersed cells were then directly resuspended in FACS buffer.

5.3. Pancreatic stromal explants in 2D-culture

Pancreatic stromal explants were separated of the epithelial cell fraction as previously described [33] with modifications. In brief, whole pancreas was minced, digested, washed, and filtered in same fashion as for the isolation of epithelial explants. Floating epithelial cell fraction was discharged 24 h after cell isolation. Cells attached to the culture flask were washed in PBS (PAA) and further cultured in PSM until 70% confluence was reached. After one passage using 0.5% trypsin (PAA) cells were resuspended in 75 cm^2 culture flasks and cultured until 90% confluence. Cells were harvested and cryoconversated in 10% DMSO/FCS (Carl Roth/PAA) at -80 °C (mean cultivation time: 18 days). Mesenchymal cells and especially fibroblasts grow much faster than epithelial cells, thus this method provides a high degree of purity of stromal cells, most of them fibroblasts. Before cryoconservation, validation of purity for pancreatic stromal cells was performed using light microscopy. For experiments, pancreatic stromal cells were thawed and viable cells were counted using Trypan Blue (Gibco) and seeded at density of 12×10^4 cells/well in the basolateral chamber of 6-well plates (BD)

in 600 μL PEM. The following day, the adhesion grade of stromal cells was evaluated and if applicable, further cultured until 70% confluency was reached (5–7 days). Cells were subjected to IFN-β treatment experiments.

5.4. In vitro IFN-β treatment

IFN-β 5×10^4 I.U/ml (Hycult Biotech) was resuspended in saline and titrated to stock solutions and stored at -80 °C. All stock solutions were only thawed once. All IFN-β treatment experiments were conducted in PEM. After treatment epithelial cells were aspirated and washed to remove IFN-β and either was used for qPCR or FACS. Stromal cells were trypsinated using 0.5% Trypsin-EDTA (PAA) for 5min at 37 °C and washed before subjected to RNA-extraction.

5.5. FACS analysis of Lin$^-$Sca-1$^+$ and Lin$^-$Sca-1$^-$c-Kit$^+$ cells

For fluorescence-activated cell sorting (FACS), antibody-labeling was performed in FACS buffer composed of PBS (PAA) containing 0.5% FCS at a cellular density of 2 × 106 cells/ml on ice for 15 min. The following antibodies were used for flow cytometry: rat-Anti-Sca-1-PE-Cy7pAK (1:500) (eBioscience), rat-Anti Sca-1-FITC pAK (eBioscience), Biotin anti-mouse Lineage Panel (Biolegend), rat-Anti-CD117(c-Kit)-PE-2B8-AK (eBioscience). Subsequently, all samples were washed twice in FACS buffer, and propidiumiodid was added at 1:200 dilutions. Stained samples were collected using a FACSAria Cell Sorting System (BD) with FACSDiva Software 6.1.2 (BD). Following negative selection for Lin$^+$ cells, remaining gated cells were sorted based on high Sca-1 and high or medium expression levels of Sca-1 and c-Kit.

5.6. RNA isolation and cDNA synthesis

Total RNA was extracted of pelleted cells using RNeasyPlusMini Kit (Quiagen) according to the manufacturer's-protocol. RNA integrity was checked by denaturing agarose gel electrophoresis. 1 μg complementary DNA was synthesized using Quantitect Reverse Transcription Kit (Quiagen).

5.7. Qualitative-PCR (RT-PCR)

RT-PCR was performed in a Thermo Cycler (Eppendorf) using Dream Taq Green PCR Master Mix (Thermo Scientific) following the manufacturer's instructions. Each PCR included a negative control for reverse transcription to exclude genomic DNA contamination. A template-free control was included to check for reagent contamination. All samples were amplified to *Gapdh/Actb* as an internal control. Amplified samples were visualized on 0.8% agarose gel using ethidium bromide (Carl Roth). The following primer-pairs were used: *α-sma* fw-ACTGGGACGACATGGAAAAG and rev-CATCTCCAGAGT CCAGCACA, *Amy* fw-TTCTGCTGCTTTCCCTCATT and rev-CATTGTTGCACCTTGTCACC, *Act-B (housekeeping)* fw-AAA CTG GAACGG TGA AGG C and rev-GCT GCCTCAACACCTCAAC, *Ca2* fw-GGA AGC GTG CGG CCT TTG and rev-GCA AGAGGC-CATGTCTGCTC, *Cftr* fw-CAGTCATCTCTGCCTTGTGG and rev-ACG CTGACCTCCACTCAGTG, *Ins* fw-TCCTGCCCCTGCTGGCCCTGC and rev-CAGTTGCAGTAGTTCTCCA, *Gapdh (housekeeping)* fw-TGGCATGATGGTCGATTCTA and rev-CACATTGGGGGTAGGAACCAC, *Ptprc* fw-CTATGGCCCTAAAACCTTTTACAT and rev-GTTGTTCATCTAAATTGCTGGATC, *Vim* fw-CGTCCTCCTACCGCAGGAT and rev-CAGTTGCAGTAGTTCTCCA. Reaction products were visualized by agarose gel electrophoresis (1.5%) (Carl Roth).

5.8. Quantitative PCR (qRT-PCR)

PCR amplification was performed with 1 μg cDNA with the LightCycler 480-system (Roche) using Light Cycler 480 Probes Master (Roche) and Universal Probe Probe Library (UPL) (Roche) according to manufacturer's instructions and the MIQUE Giudelines [44]. For UPL-assays 400 nM fw- and rev-Primer was used together with 100 nM Universal Probe Library Probe (Roche) in a final Volume of 25 μl. Ifnar-1 was amplified using SYBR Green 1 Master kit (Roche). PCR reactions were run in doublets for 40 cycles consisting of 15 s denaturation at 95 °C, primer annealing for 15 s at 55 °C, and extension for 15 s at 72 °C. The sequences of applied primer sets in the UPL assays were as following: *Aldh1A1* fw-CGGATTTAGGAGGCTGCATA and rev-TTGTATAAGTGAAAATGTCTCCATCA (UP #26), *c-Kit* fw-GGAGCCCA CAATAGATTGGTA and rev-CACTGGTGAGACAGGAGTGG (UP #68), *C-met* fw-CCACCCGACCAAATCTTT and rev-GCTAACCGAGTT CAGGGTCTT (UP #31), *Cxcl-10* fw-AATGAAAGCGTTTAG CCAAAA and rev-AGGGGAGTGATGGAGAGAGG (UP #56), *Nestin* fw-TGCAGGCCACTGAAAAGTT and rev-TTCCAGGATCTGAGCGATCT (UP #2), *Pdx1* fw-GAAATCCACCAAAGCTCACG and rev-CGGGTTCCGC TGTGTAAG (UP #51), *Ptf1a* fw-CACCGACCAGTCCTCTCG and rev-AACTCTACTTCTGCTTGCTCGT (UP #3), *Ppib (housekeeping)* fw-TCCACCTTCCGTACCACATC and rev-GAGGCCATTTGGGAACTTCT (UP #20), *Rpl13a (housekeeping)* fw-CCCTCCACCCTATGACAA and rev-GTAGGCTTCAGCCGACA (UP #108), *Sca-1* fw-CCCCTACCCTGA TGGAGTCT and rev-TGTTCTTTACTTTCCTTGTTTGAGAA (UP #16). The sequences of the applied primer set for Ifnar-1 was fw-CCGGCCTCCCAAGACGATGC and rev-TCTCCACCTGCAGCTGAGGGT. Obtained data was analyzed using the ΔΔct-method to calculate target gene levels in comparison to mean values of internal control genes of *Ppib* and *Rpl13* as described earlier [45].

5.9. Pancreatosphere formation assay

For quantitative pancreatosphere formation assays on sorted Lin$^-$Sca-1$^+$ and Lin$^-$Sca-1$^+$c-Kit$^+$ cells were performed by plating cells in 24-well ultra-low attachment plates (Corning) at densities of 100, 1000, 2400 cells per well (0,2 cells/μL, 2 cells/μL, 4,8 cells/μL) in PMM, well diameter approx. 1.9 cm^2. Cells were grown 6 days if not stated otherwise, and sphere formation was quantified using an Axiovert 40 CFL microscope (Carl Zeiss) by calculating the mean value of counts from spheres reaching a minimal diameter 100 μm conducted by two independent researchers. All sphere formation experiments were held in quadruplicate and performed three times. To prevent evaporation loss over the time course, 125 μl of fresh PMM was added in each well every day. The medium was changed every 3 days. Serial passages were performed by dissociating spheres using the NeuroCult Chemical Dissociation Kit (StemCell Technologies).

5.10. Lin$^-$Sca-1$^+$ 3D-culture

This was used for immunofluorescence analysis of Lin$^-$Sca-1$^+$ Spheres. Sorted Lin$^-$Sca-1$^+$ and Lin$^-$Sca-1$^+$ c-Kit $^+$ cells were resuspended in PMM and Matrigel™ (25:1) (BD) and seeded on media chamber slides Millicell™ EZ SLIDES (Merck-Millipore) coated with 40 μl Matrigel™. Matrigel™-coated slides were incubated for 30 min at 37 °C and 5% CO2 in forehand for Matrigel™-Polymerization. The culture period was 5–14 days before subjected to immunofluorescence analysis. Light microscopic pictures were taken with an Axioscope Zeiss microscope (Zeiss).

5.11. Histology, immunohistochemistry, and immunofluorescence

Immunohistochemistry staining was performed using affinity-

purified polyclonal antibody rat-Anti-Sca-1 (Abcam) and for dual-Staining antibodies and rabbit-Anti-Ck-19 (DSHB-University of Iowa). For Immunofluorescence of Matrigel™-coated slides primary antibodies were rat-Anti-Sca-1 (Abcam), rabbit-Anti- c-Kit (Abcam), rabbit-Anti-Amylase (Santa Cruz Biotechnology), rat-Anti-E-Cadherin (DECMA-1), rabbit-Anti-Ck 19 (Abcam), rat-Anti-Nestin (Abcam) and goat-anti-rat Alexa Fluor 488 (Cell Signaling Technology), donkey-anti-rabbit Alexa Fluor 488 nm (MolecularProbes), donkey-anti-rabbit Alexa Fluor 555 nm (Cell Signaling Technology) for secondary antibodies and counterstained with the DNA-binding dye DAP. For immunofluorescence staining of WT, AP, and $Kras^{G12D}$ FFPE, primary antibodies were Anti-Sca-1 (Abcam) and Anti-pStat-1 (Cell Signaling), and Alexa Fluor 568 Goat anti-Rat and Alexa Fluor 488 Goat anti-Rabbit secondary antibodies, and counterstained with the DNA-binding dye DAPI.

Acknowledgements

The authors thank Manja Thorwirth and Isabell Schäffer for their excellent technical support. We are grateful to Florian and Max Leinenkugel for comments and illustrations that improved the manuscript. We also thank Judith Lamb for spell checking. The project was funded by a grant of the Deutsche Forschungsgemeinschaft (Project No. 216005011).

References

[1] Offield MF, Jetton TL, Labosky PA, Ray M, Stein RW, Magnuson MA, et al. Pdx-1 is required for outgrowth and differentiation of the rostral duodenum. Development 1996;122:983–95.
[2] Gradwohl G, Dierich A, LeMeur M, Guillemot F. Neurogenin3 is required for the development of the four endocrine cell lineages of the pancreas. Proc Natl Acad Sci U S A 2000;97:1607–11.
[3] Spence JR, Wells JM. Translational embryology: using embryonic principles to generate pancreatic endocrine cells from embryonic stem cells. Dev Dynam 2007;236:3218–27.
[4] Schwitzgebel VM, Scheel DW, Conners JR, Kalamaras J, Lee JE, Anderson DJ, et al. Expression of neurogenin3 reveals an islet cell precursor population in the pancreas. Development 2000;127:3533–42.
[5] Apelqvist A, Li H, Sommer L, Beatus P, Anderson DJ, Honjo T, et al. Notch signalling controls pancreatic cell differentiation. Nature 1999;400:877–81.
[6] Stanger BZ, Hebrok M. Control of cell identity in pancreas development and regeneration. Gastroenterology 2013;144:1170–9.
[7] Strobel O, Dor Y, Alsina J, Stirman A, Lauwers G, Trainor A, et al. In vivo lineage tracing defines the role of acinar-to-ductal transdifferentiation in inflammatory ductal metaplasia. Gastroenterology 2007;133:1999–2009.
[8] Kopp JL, von Figura G, Mayes E, Liu FF, Dubois CL, Morris JPt, et al. Identification of sox9- dependent acinar-to-ductal reprogramming as the principal mechanism for initiation of pancreatic ductal adenocarcinoma. Cancer Cell 2012;22:737–50.
[9] Guerra C, Schuhmacher AJ, Canamero M, Grippo PJ, Verdaguer L, Perez-Gallego L, et al. Chronic pancreatitis is essential for induction of pancreatic ductal adenocarcinoma by k-ras oncogenes in adult mice. Cancer Cell 2007;11:291–302.
[10] Carriere C, Young AL, Gunn JR, Longnecker DS, Korc M. Acute pancreatitis markedly accelerates pancreatic cancer progression in mice expressing oncogenic kras. Biochem Biophys Res Commun 2009;382:561–5.
[11] Kong B, Bruns P, Behler NA, Chang L, Schlitter AM, Cao J, et al. Dynamic landscape of pancreatic carcinogenesis reveals early molecular networks of malignancy. Gut 2018;67:146–56.
[12] Hingorani SR, Petricoin EF, Maitra A, Rajapakse V, King C, Jacobetz MA, et al. Preinvasive and invasive ductal pancreatic cancer and its early detection in the mouse. Cancer Cell 2003;4:437–50.
[13] Dor Y, Brown J, Martinez OI, Melton DA. Adult pancreatic beta-cells are formed by self- duplication rather than stem-cell differentiation. Nature 2004;429:41–6.
[14] Desai BM, Oliver-Krasinski J, De Leon DD, Farzad C, Hong N, Leach SD, et al. Preexisting pancreatic acinar cells contribute to acinar cell, but not islet beta cell, regeneration. J Clin Invest 2007;117:971–7.
[15] Clayton HW, Osipovich AB, Stancill JS, Schneider JD, Vianna PG, Shanks CM, et al. Pancreatic inflammation redirects acinar to beta cell reprogramming. Cell Rep 2016;17:2028–41.
[16] Gu G, Dubauskaite J, Melton DA. Direct evidence for the pancreatic lineage: Ngn3+ cells are islet progenitors and are distinct from duct progenitors. Development 2002;129:2447–57.
[17] Shroff S, Rashid A, Wang H, Katz MH, Abbruzzese JL, Fleming JB, et al. Sox9: a useful marker for pancreatic ductal lineage of pancreatic neoplasms. Hum Pathol 2014;45:456–63.
[18] Rovira M, Scott SG, Liss AS, Jensen J, Thayer SP, Leach SD. Isolation and characterization of centroacinar/terminal ductal progenitor cells in adult mouse pancreas. Proc Natl Acad Sci U S A 2010;107:75–80.
[19] Sato T, Onai N, Yoshihara H, Arai F, Suda T, Ohteki T. Interferon regulatory factor-2 protects quiescent hematopoietic stem cells from type i interferon-dependent exhaustion. Nat Med 2009;15:696–700.
[20] Essers MA, Offner S, Blanco-Bose WE, Waibler Z, Kalinke U, Duchosal MA, et al. Ifnalpha activates dormant haematopoietic stem cells in vivo. Nature 2009;458:904–8.
[21] Gallmeier E, Schafer C, Moubarak P, Tietz A, Plossl I, Huss R, et al. Jak and stat proteins are expressed and activated by ifn-gamma in rat pancreatic acinar cells. J Cell Physiol 2005;203:209–16.
[22] Morcos MNF, Schoedel KB, Hoppe A, Behrendt R, Basak O, Clevers HC, et al. Sca-1 expression level identifies quiescent hematopoietic stem and progenitor cells. Stem Cell Rep 2017;8:1472–8.
[23] Holmes C, Stanford WL. Concise review: stem cell antigen-1: expression, function, and enigma. Stem Cell 2007;25:1339–47.
[24] Lawson DA, Xin L, Lukacs RU, Cheng D, Witte ON. Isolation and functional characterization of murine prostate stem cells. Proc Natl Acad Sci U S A 2007;104:181–6.
[25] Dekel B, Zangi L, Shezen E, Reich-Zeliger S, Eventov-Friedman S, Katchman H, et al. Isolation and characterization of nontubular sca-1+lin- multipotent stem/progenitor cells from adult mouse kidney. J Am Soc Nephrol 2006;17:3300–14.
[26] Welm BE, Tepera SB, Venezia T, Graubert TA, Rosen JM, Goodell MA. Sca-1(pos) cells in the mouse mammary gland represent an enriched progenitor cell population. Dev Biol 2002;245:42–56.
[27] Grange C, Lanzardo S, Cavallo F, Camussi G, Bussolati B. Sca-1 identifies the tumor-initiating cells in mammary tumors of balb-neut transgenic mice. Neoplasia 2008;10:1433–43.
[28] Samuelson L, Wright N, Gerber DA. Endodermal progenitor cells isolated from mouse pancreas. Stem Cell Discov 2011;1(3):10.
[29] Ma F, Chen F, Chi Y, Yang S, Lu S, Han Z. Isolation of pancreatic progenitor cells with the surface marker of hematopoietic stem cells. Internet J Endocrinol 2012;2012:948683.
[30] Seaberg RM, Smukler SR, Kieffer TJ, Enikolopov G, Asghar Z, Wheeler MB, et al. Clonal identification of multipotent precursors from adult mouse pancreas that generate neural and pancreatic lineages. Nat Biotechnol 2004;22:1115–24.
[31] Morris JPt, Cano DA, Sekine S, Wang SC, Hebrok M. Beta-catenin blocks kras-dependent reprogramming of acini into pancreatic cancer precursor lesions in mice. J Clin Invest 2010;120:508–20.
[32] Means AL, Meszoely IM, Suzuki K, Miyamoto Y, Rustgi AK, Coffey Jr RJ, et al. Pancreatic epithelial plasticity mediated by acinar cell transdifferentiation and generation of nestin- positive intermediates. Development 2005;132:3767–76.
[33] Bachem MG, Schneider E, Gross H, Weidenbach H, Schmid RM, Menke A, et al. Identification, culture, and characterization of pancreatic stellate cells in rats and humans. Gastroenterology 1998;115:421–32.
[34] Jost E, Roos WP, Kaina B, Schmidberger H. Response of pancreatic cancer cells treated with interferon-alpha or beta and co-exposed to ionising radiation. Int J Radiat Biol 2010;86:732–41.
[35] Gorelick FSAG, Kern HF. Cerulein-induced pancreatitis. Vl go, ep dimagno, jd gardner, e lebenthal, ha reber, ga scheele. In: The pancreas: biology, pathobiology and disease. second ed. New York: Raven Press; 1993. p. 501–26.
[36] Jensen JN, Cameron E, Garay MV, Starkey TW, Gianani R, Jensen J. Recapitulation of elements of embryonic development in adult mouse pancreatic regeneration. Gastroenterology 2005;128:728–41.
[37] Marshall 2nd GP, Ross HH, Suslov O, Zheng T, Steindler DA, Laywell ED. Production of neurospheres from cns tissue. Methods Mol Biol 2008;438:135–50.
[38] Kong B, Michalski CW, Erkan M, Friess H, Kleeff J. From tissue turnover to the cell of origin for pancreatic cancer. Nat Rev Gastroenterol Hepatol 2011;8:467–72.
[39] Ku HT. Minireview: pancreatic progenitor cells–recent studies. Endocrinology 2008;149:4312–6.
[40] Gasslander T, Ihse I, Smeds S. The importance of the centroacinar region in cerulein-induced mouse pancreatic growth. Scand J Gastroenterol 1992;27:564–70.
[41] Mulholland DJ, Xin L, Morim A, Lawson D, Witte O, Wu H. Lin-sca-1+cd49fhigh stem/progenitors are tumor-initiating cells in the pten-null prostate cancer model. Cancer Res 2009;69:8555–62.
[42] Bamezai A. Mouse Ly-6 proteins and their extended family: markers of cell differentiation and regulators of cell signaling. Arch Immunol Ther Exp (Warsz). 2004 Jul-Aug;52(4):255–66.
[43] Upadhyay G. Emerging role of novel biomarkers of Ly6 gene family in Pan cancer. Adv Exp Med Biol 2019;1164:47–61.
[44] Bustin SA, Benes V, Garson JA, Hellemans J, Huggett J, Kubista M, et al. The miqe guidelines: minimum information for publication of quantitative real-time pcr experiments. Clin Chem 2009;55:611–22.
[45] Pfaffl MW. A new mathematical model for relative quantification in real-time rt-pcr. Nucleic Acids Res 2001;29:e45.